

Research Article

Cite this article: Pramneechote P, Chotikarn P, Thammakeerati N, Heembo M and Sinutok S (2025) Differences in thermal sensitivities and thermal performance curves of the three calcifying macroalgae *Padina boryana*, *Halimeda opuntia*, and *Halimeda macroloba*. *Journal of the Marine Biological Association of the United Kingdom* **105**, e42, 1–16. <https://doi.org/10.1017/S0025315425000359>

Received: 25 November 2024

Revised: 13 March 2025

Accepted: 17 March 2025

Keywords:

climate change, elevated temperature, heat stress, metabolism, photosynthetic performance

Corresponding author:

Sutinee Sinutok;

Email: ssutinee@gmail.com

© The Author(s), 2025. Published by Cambridge University Press on behalf of Marine Biological Association of the United Kingdom. This is an Open Access article, distributed under the terms of the Creative Commons Attribution licence (<http://creativecommons.org/licenses/by/4.0>), which permits unrestricted re-use, distribution and reproduction, provided the original article is properly cited.



Differences in thermal sensitivities and thermal performance curves of the three calcifying macroalgae *Padina boryana*, *Halimeda opuntia*, and *Halimeda macroloba*

Pathompong Pramneechote^{1,2}, Ponlachart Chotikarn^{1,2},
Natthida Thammakeerati^{1,2}, Muhammad Heembo^{1,2} and Sutinee Sinutok^{1,2} 

¹Faculty of Environmental Management, Prince of Songkla University, Hat Yai, Songkhla, Thailand and ²Coastal Oceanography and Climate Change Research Center, Prince of Songkla University, Hat Yai, Songkhla, Thailand

Abstract

Calcifying macroalgae play a critical role in coastal ecosystems, but rising sea temperatures pose a significant threat to their survival. This study aims to investigate the thermal sensitivity of the three marine macroalgal species *Padina boryana*, *Halimeda opuntia*, and *H. macroloba*. Photosynthetic performance, metabolism, pigment content, and oxidative stress-related parameters were measured at temperatures of 28°C, 32°C, 36°C, and 40°C and the thermal performance curves (TPCs) were determined for F_v/F_m , F_v/F_0 , ϕ PSII, and oxygen production to assess maximum rate (R_{max}), optimum temperature (T_{opt}), critical thermal maximum (CT_{max}), and thermal safety margin (TSM) of these three macroalgal species. The results showed that 40°C had the most negative effect on all three species with *P. boryana* demonstrating better performance compared to both *Halimeda* species. TPCs from photosynthetic performance revealed thermal sensitivity variations by species and *P. boryana* exhibited a broader thermal tolerance range compared to *Halimeda*. On the other hand, TPCs of oxygen production provided similar CT_{max} values. Based on TPC projections, all three species might survive future ocean warming and marine heatwaves, though these conditions will have significant effects, with *P. boryana* showing greater tolerance than both *Halimeda* species. This study highlights the differential thermal responses and sensitivities of these macroalgae, contributing to understanding their potential resiliencies under future climate change scenarios.

Introduction

Marine macroalgae play a key role in coastal ecosystems since they contribute to primary production, nutrient cycling, and provide habitats for other marine organisms (Hall *et al.*, 2022; Jacobs *et al.*, 2023). To survive in their habitat, macroalgae must handle numerous environmental stressors that result from changes of environmental factors such as light, temperature, oxygen, carbon, pH, and nutrients (Ji and Gao, 2023). With global warming, the exposure to these stressors is becoming more severe and longer, resulting in a higher level of impact on coastal communities, especially due to high temperatures (Graba-Landry *et al.*, 2020; Wu *et al.*, 2022). Generally, temperature of seawater is a factor that relates to the distribution of marine living organisms since it has a large effect on the metabolism rate of the organism, and an extremely high temperature is a significant stressor that can severely disrupt the physiological processes of every marine organism (Graba-Landry *et al.*, 2020). In photosynthetic organisms, high temperatures impair critical photosynthesis enzymes and increase electrolyte leakage, resulting in a reduction of photosynthetic efficiency and increasing the production rate of reactive oxygen species (ROS) (Das and Roychoudhury, 2014; Ji and Gao, 2023). This accumulation of ROS leads to biomolecule degradation and cellular dysfunction, and at worst it may lead to programmed cell death (Clark *et al.*, 2013; Fernández *et al.*, 2020; Ji and Gao, 2023). To mitigate these impacts, marine macroalgae have shown a remarkable capacity for acclimation, involving many adjustments to their physiological, biochemical, and morphological traits (Barati *et al.*, 2019; Chintakovid *et al.*, 2024; Díaz-Acosta *et al.*, 2021; Ji and Gao, 2023).

Calcifying marine macroalgae, or calcareous algae, compose a functional group of marine macroalgae from diverse clades that shared the characteristics of calcification, a biogenic precipitation of calcium carbonate ($CaCO_3$) (Nelson, 2009; Scherner *et al.*, 2016). Calcium carbonate crystals are then stored in their cells or between the cells, depending on the species (Borowitzka and Larkum, 1987). The shape of calcium carbonate crystals has been used to classify them into

two groups: aragonite and calcite (Borowitzka and Larkum, 1987). Calcium carbonate crystals contribute significantly to structural support and defence against herbivores by making them less appetising (Campbell *et al.*, 2014). In the context of ecosystem service, this calcification provides additional services as reef builders and stabilizers (Nelson, 2009). However, many studies show that calcifying algae might be sensitive to global warming conditions, especially to an elevated temperature and ocean acidification (Buapet and Sinutok, 2023; Campbell *et al.*, 2014; Hofmann *et al.*, 2012; Ji and Gao, 2023). High temperatures impair calcification of calcifying algae through reducing the photosynthesis rate, which is closely coupled with calcification. This coupling arises from the pH increase in the microenvironment during photosynthesis, changing the carbon balance toward increased CO_3^{2-} , which is essential for calcifying (Buapet and Sinutok, 2021, 2023). Ocean acidification reduces net calcification rates since it increases calcium carbonate dissolution rates (McNicholl *et al.*, 2020). As a result, the calcifying algae will have less competitive advantage and might lose their area cover in future seawater conditions (Kram *et al.*, 2016; Nelson, 2009). Conversely, non-calcifying algae are usually less affected or even benefit from these conditions (Hofmann *et al.*, 2012; Liu *et al.*, 2018).

To forecast species composition and the functioning of coastal communities in the elevated temperature situation, it is essential to understand the thermal sensitivity of each organism in the habitat (Duarte *et al.*, 2018). Thermal sensitivity of macroalgae was found to vary by species, population, site, life stage, and life history (Fredersdorf *et al.*, 2009; Savva *et al.*, 2018; Wieters *et al.*, 2013; Zou and Gao, 2013). Moreover, thermal sensitivity is also influenced by many other physical environmental factors, such as light intensity, light quality, salinity, pH, and CO_2 concentration (Koch *et al.*, 2013; Liu *et al.*, 2018; Rautenberger *et al.*, 2015; Zou *et al.*, 2018). Consequently, an *ex situ* experiment is used to exclude the effects of other environmental factors when investigating thermal sensitivity. One of the common approaches to this is to construct the thermal performance curve (TPC) (Deutsch *et al.*, 2008; Schulte *et al.*, 2011; Sinclair *et al.*, 2016; Vasseur *et al.*, 2014). A TPC is a curve that shows a performance parameter of an individual or a population in response to the change in environmental temperature (Low-Décarie *et al.*, 2017). Performance parameters in TPCs studies vary among growth rate, population growth rate, heart rate, respiration rate, and photosynthesis, depending on species and duration of the experiment (Low-Décarie *et al.*, 2017). TPC studies on macroalgae frequently use growth rate, respiration rate, and photosynthesis (Anton *et al.*, 2020; Bennett *et al.*, 2022; Díaz-Acosta *et al.*, 2021). However, since the TPC curve is usually asymmetric, it is difficult to choose a formula that is adequate for modelling (Deutsch *et al.*, 2008). Moreover, this curve varies largely across species and chosen performance parameter, so there is no universal model that works best for all studies (Low-Décarie *et al.*, 2017; Rebolledo *et al.*, 2021). Consequently, each study chooses a specific model depending mainly on the data characteristics from its experiments (Low-Décarie *et al.*, 2017; Rebolledo *et al.*, 2021). Fitting a model to TPCs provides several comparable parameters that reveal the thermal characteristics of organisms, including lower critical thermal limits (CT_{\min}), upper critical thermal limits (CT_{\max}), thermal optimum (T_{opt}), and thermal safety margin (TSM) (Angilletta *et al.*, 2010; Silbiger *et al.*, 2019). Changes in these parameters indicate the ability to acclimate (Crous *et al.*, 2022). The differences among them are used to examine both interspecies and intraspecies variations in thermal characteristics (Anton *et al.*, 2020; Silbiger *et al.*, 2019).

In shallow coastal areas, seawater temperature shifts mainly due to the rhythms of tidal and diel cycles. With global warming increasing sea surface temperature (SST) and the occurrence of marine heatwaves (MHWs), the intensity and duration of high temperatures during the day may increase in these areas (Wiberg, 2023). Therefore, understanding the thermal sensitivity of shallow water macroalgae is essential. However, there is a knowledge gap in understanding the responses of specific shallow-water calcifying macroalgal species to high-temperature conditions (Nelson, 2009). In this study, we examined the thermal sensitivity and thermal responses of three calcifying macroalgae, *Padina boryana*, *Halimeda opuntia*, and *H. macroloba*, which are common and coexist along the coast of Thailand. We also constructed TPCs for these species to extrapolate the effects of high temperatures, with the motivation that the results of this study might provide insights to effects on coastal communities in the global warming era.

Materials and methods

Sample collection and acclimation

Thalli and holdfasts of *Padina boryana*, *Halimeda macroloba*, and *H. opuntia* were collected from Tang Khen Bay, Phuket, Thailand (7.811 N, 98.404 E) (Figure 1). These macrophytes inhabit the low intertidal zone, where they are exposed to air during low tide in spring tides. Samples were selected and then kept in a container with seawater from the sampling site. The samples were transferred to the aquaria facility of the Coastal Oceanography and Climate Change Research Center, Prince of Songkla University, within 10 h.

Before the experiment, samples were then acclimated for 3 days in 15-L aquariums containing filtered seawater with a salinity of 33 PSU and a pH of 8.2. The irradiance setting was 200 $\mu\text{mol photons m}^{-2} \text{ s}^{-1}$ (A601, Chihiros, China) at canopy height with a 12:12 h dark–light cycle. The temperature at the aquaria facility was in the range of 27–32°C. All parameter settings were based on an average *in situ* value. During acclimation, the seawater was renewed daily.

Experimental design

Effect of temperature on photosynthesis parameters, total ROS level, and ROS scavenging enzyme

In this study, there were four target temperatures (28°C, 32°C, 36°C, and 40°C). The highest target temperature (40°C) and the 12-h stress phase were chosen to reflect a potential stress condition of seawater temperature during low tide in tropical shallow coastal areas. A previous experiment recorded a maximum *in situ* temperature of 42°C at the same study site (Yucharoen *et al.*, 2021), supporting the selection of 40°C as the highest target temperature. The irradiance level in this study was 200 $\mu\text{mol photons m}^{-2} \text{ s}^{-1}$ at canopy height, which was chosen based on average *in situ* irradiance (Yucharoen *et al.*, 2021).

Four aquarium tanks (15 L) were used in this study, each tank for a target temperature. Inside each aquarium tanks, four biological replicates for each species were put separately in small tanks (1 L) to rule out the interaction among individual organisms. Each small tank was filled with filtered seawater (33 PSU) with a compressed air pump. The salinity of seawater was checked every 12 h and maintained by adding distilled water. In the acclimation phase, the temperature of each aquarium tank was controlled at 28°C for 24 h. In the ramping phase, seawater temperature was ramped up at a rate of 2°C every 4 h until it reached the target temperature of

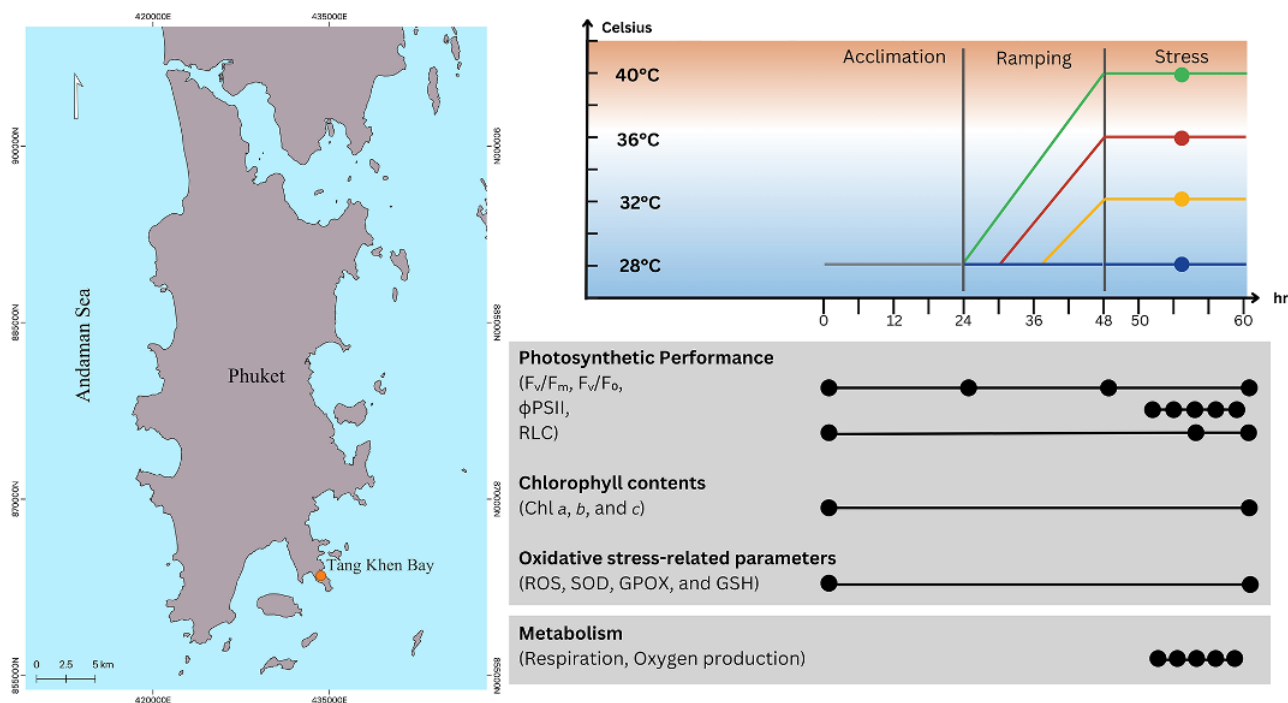


Figure 1. Study site and a diagram showing the timeline for parameters investigated in this study.

each tank (Marín-Guirao *et al.*, 2017). To let all tanks reach their target temperature simultaneously, the tank with the highest target temperature (40°C) was ramped first. Other tanks began ramping later, so they also reached their target temperatures at 48 h of the experiment. The last phase was the stress phase, where the temperature of each tank was maintained at its target temperature for 12 h (Figure 1). The 12:12 h dark–light cycle was also applied during experiment, with light turning on at 0, 24, and 48 h of experiment and turning off at 12, 36, and 60 h of experiment.

The maximum quantum yield (F_v/F_m) and the potential activity of Photosystem II (PSII) (F_v/F_0) were measured at the start of the experiment, before the ramping phase (24 h of experimental period), after the ramping phase (48 h of experimental period), and at the end of the experiment (60 h of experimental period). The effective quantum yield (ϕ PSII) was measured at 2, 4, 6, 8, and 10 h of the stress phase when the temperature was steady ($n = 4$). Lastly, rapid light curves (RLCs) were measured at the start of the experiment, and at 6, and 12 h of the stress phase when the temperature was steady (54 and 60 h of the experimental period) (Figure 1). All fluorescence measurements were accessed in three areas for each individual ($n = 12$) except the RLCs which were collected in one area ($n = 4$).

At the end of the experiment, samples were rapidly frozen in liquid nitrogen and subsequently preserved in a -80°C freezer for future analysis of oxidative stress–related parameters (total ROS content, superoxide dismutase [SOD] activity, guaiacol peroxidase [GPOX] activity, and glutathione [GSH] content) ($n = 4$ –12) and pigment concentrations (chlorophyll *a*, *b*, and *c*) ($n = 4$) (Figure 1).

Effect of temperature on metabolism

The metabolism experiment was separately performed using the same aquarium setting as in the photosynthesis performance experiment, where each aquarium tank is for a specific target temperature. However, in this experiment, each species had eight

individuals per aquarium tank, with four biological replicates being placed individually inside glass chambers (exposed to light) and four biological replicates being placed individually inside dark chambers (non-exposed to light). In addition, during the ramping phase, temperature was increased at a rate of 2°C per 2 h (Zanolla *et al.*, 2019). The oxygen level of seawater in each glass chamber was measured initially and at 4 h of the stress phase at steady temperature. The change in oxygen level in glass chambers was used for assessing the net oxygen production ($n = 4$) and the change in the dark chambers was used for assessing the respiration ($n = 4$) (Figure 1).

Chlorophyll fluorescence parameters

The evaluation of PSII chlorophyll fluorescence parameters was conducted using a Pulse Amplitude Modulated Fluorometer (Diving-PAM, Walz, Effeltrich, Germany), coupled with a 6-mm diameter fibre optic probe. An Underwater Adapter (DIVING-DA) was equipped with the fibre optic probe to ensure the consistency of the distance between the probe and sample.

F_v/F_m and F_v/F_0 were determined in a single measurement in the dark. These two parameters show the maximum potential ratio of PSII to capture light energy. However, F_v/F_0 had higher sensitivity than F_v/F_m (Babani and Lichtenthaler, 1996). F_v/F_m was calculated as $(F_m - F_0)/F_m$, while F_v/F_0 was calculated as $(F_m - F_0)/F_0$. Here, F_0 represents the minimum fluorescence emitted after being dark-adapted, while F_m represents the maximum fluorescence emitted following a saturating pulse (Babani and Lichtenthaler, 1996).

ϕ PSII was measured on actinic light, determining the ratio of capturing light to the photochemistry of PSII on the actinic light (Schreiber, 2004). ϕ PSII was determined using the formula $(F'_m - F)/F'_m$, where F represents the minimum fluorescence emitted in the light-adapted stage and F'_m represents the maximum

fluorescence attained after applying a saturating pulse (Schreiber, 2004).

The RLC was determined after dark adaptation for 15 min. The light pulse setting was at 11 intensities (0, 43, 63, 87, 121, 183, 276, 406, 608, 795, and 1112 $\mu\text{mol photons m}^{-2} \text{s}^{-1}$) with each light pulse being applied for 20 s. The RLC parameters, including initial slope of RLC (α), minimum saturating irradiance (E_k), and maximum electron transport rate (ETR_{max}) were extracted from RLC, following Ralph and Gademann (2005).

Metabolism

Oxygen concentration measurement was conducted by use of Fibox 4 with a polymer optical fibre and an oxygen sensor spot (SP-PSt3-YAU-D5-YOP, Presens GmbH, Germany) attached inside the chamber. During measurement, a magnetic stirrer (MS300HS, M TOPS, Korea) was used to maintain uniform oxygen levels in the seawater. Oxygen production and respiration rate were calculated using the formula $[(\text{DO})_{\text{final}} - (\text{DO})_{\text{initial}}]/[(\text{T})_{\text{final}} - (\text{T})_{\text{initial}}]$ following Olivé *et al.* (2016). The metabolic rate was normalized by the wet weight and corrected using the chambers that did not contain algae.

Pigment contents

Photosynthetic pigment concentrations were quantified employing the spectrophotometric technique (Ritchie, 2006). Chlorophyll pigments were extracted through the homogenisation of macroalgal tissue in 4 ml of 90% acetone maintained in the dark at 4°C for 24 h. Subsequently, the solution was centrifuged at 1,500 g for 10 min. The supernatant absorbance was then measured at wavelengths of 630, 647, 664, and 750 nm using a spectrophotometer (FP-8200, JASCO, Japan). Chlorophyll contents of *P. boryana* were calculated using formulae for phaeophytes (Equations 1 and 2), and chlorophyll contents of *H. opuntia* and *H. macroloba* were calculated using formulae for chlorophytes (Equations 3 and 4) (Ritchie, 2006). Chlorophyll concentration was normalized with surface area (cm^2) for *P. boryana* and with fresh weight (g) for *H. opuntia* and *H. macroloba*.

$$\begin{aligned} \text{Chlorophyll } a &= [-0.45 \times (\text{A}_{630} - \text{A}_{750} \text{ nm})] \\ &+ [11.49 \times (\text{A}_{664} - \text{A}_{750} \text{ nm})] \end{aligned} \quad (1)$$

$$\begin{aligned} \text{Chlorophyll } c &= [22.679 \times (\text{A}_{630} - \text{A}_{750} \text{ nm})] \\ &+ [-3.404 \times (\text{A}_{664} - \text{A}_{750} \text{ nm})] \end{aligned} \quad (2)$$

$$\begin{aligned} \text{Chlorophyll } a &= [-1.786 \times (\text{A}_{647} - \text{A}_{750} \text{ nm})] \\ &+ [11.867 \times (\text{A}_{664} - \text{A}_{750} \text{ nm})] \end{aligned} \quad (3)$$

$$\begin{aligned} \text{Chlorophyll } b &= [18.978 \times (\text{A}_{647} - \text{A}_{750} \text{ nm})] \\ &+ [-4.895 \times (\text{A}_{664} - \text{A}_{750} \text{ nm})] \end{aligned} \quad (4)$$

Oxidative stress-related parameters

ROS content was determined using an adapted DCF assay following Saewong *et al.* (2022). Macroalgal tissue (100 mg) was homogenized with 1 ml of 10 mM Tris-HCl solution (pH 7.2). Subsequently, the mixture was subjected to centrifugation at

12,000 g for 20 min at 4°C. The supernatant (100 μl) was added with 10 μl of 10 mM 2',7'-dichlorofluorescein diacetate (Sigma-Aldrich, USA). The fluorescence signal after 10 min of incubation in darkness was assessed using a fluorescence spectrophotometer (FP-8200, JASCO, Japan) with an excitation wavelength of 504 nm and an emission wavelength of 524 nm. The intensity of the fluorescence signal determined the total ROS content within the sample.

SOD activity was evaluated using the nitroblue tetrazolium (NBT) technique following Saewong *et al.* (2022). Ground macroalgal tissue (100 mg) was mixed with 1 ml of extraction buffer (0.2 mM potassium phosphate buffer (pH 7.8) and 0.1 mM ethylenediaminetetraacetic acid [EDTA]). Afterward, the mixture was centrifuged at 12,000 g for 20 min at 4°C. Subsequently, 10 μl of the supernatant was added to 200 μl of reaction buffer (50 mM phosphate buffer (pH 7.8), 2 mM EDTA, 9.9 mM L-methionine, 55 μM NBT, and 0.025% v/v Triton-X100) with the addition of 2 μl of 1 mM riboflavin in microplates. On one microplate, the reaction was initiated by exposing them to light for 10 min (fluorescence, 15 W, Philips, Thailand), while the other was kept in the dark as a no-reaction treatment. Subsequently, the absorbance at 560 nm was measured using a spectrophotometer (Biotek, Vermont, USA) to determine the formazan content after the reaction. In parallel, control measurements were conducted like those above, but without the presence of macroalgal extract. SOD activity was assessed by the ability of SOD to compete with NBT for radicals, reducing the production of formazan.

GPOX activity was assessed using the technique of Phandee *et al.* (2022). Ground macroalgal tissue (100 mg) was mixed with 2 ml of an extraction buffer (0.1 M Tris-HCl containing 8.75% w/v PVPP, 0.1 M KCl, and 0.28% v/v TritonX100). Next, the mixture was centrifuged at 1,520 g for 30 min at 4°C. The reaction was initiated by mixing 50 μl of the supernatant with 230 μl of the reaction mixture (50 mM potassium phosphate buffer pH 6.6 containing 1% v/v guaicol and 0.18% v/v H_2O_2). The slope of the absorbance at 470 nm during 5 min of the reaction, which indicates GPOX activity, was assessed using a spectrophotometer (Biotek, Vermont, USA).

GSH content was assessed using a technique by Nualla-ong *et al.* (2020). Ground macroalgal tissue (100 mg) was added to a solution of 200 μl of 25% w/v meta-phosphoric acid (HPO_3) and 1.1 ml of ice-cold extraction buffer (0.1 M sodium phosphate buffer (pH 8.0) containing 5 mM EDTA). The mixture was then centrifuged at 12,000 g at a temperature of 4°C for 20 min. Subsequently, 90 μl of the supernatant was mixed with 1.62 ml of extraction buffer. The reaction was then initiated by adding 90 μl of 7.46 mM o-phthalaldehyde (OPT) to the mixture. The GSH content was determined from the fluorescence signal using a spectrophotometer (FP-8200, JASCO, Japan) with an excitation wavelength of 420 nm and an emission wavelength of 350 nm.

Thermal performance curve

A TPC, a continuous nonlinear curve between physiological performance and temperature, was used to assess and predict the impact of temperature on physiological performance. Photosynthetic performance and metabolism rates were assumed to respond to temperature with a gradual increase together, peak at the optimum temperature (T_{opt}), and then rapidly drop as temperatures surpassed T_{opt} . The photosynthesis performance data (F_v/F_m , F_v/F_0 , and ϕPSII) were used to fit with TPC models derived from the latest time measurement. The metabolism data (the net oxygen

production rate and respiration rate) were calculated from the average oxygen level production between the stress phase experimental period.

The maximum of hourly average SST in their habitat was obtained from the GHRSSST Level 4 MUR Global Foundation Sea Surface Temperature Analysis (v4.1) (J P L Mur MEASURE Project, 2015). The predicted temperature increase was based on simulations using a low-ECS model under the SSP5-8.5 scenario, which represents a worst-case, no-policy scenario predicting a 3.74°C rise by 2100 (Scafetta, 2024). To estimate the future maximum temperature for 2100, we added the predicted temperature increase to the current maximum temperature. The maximum intensity of MHWs in the worst-case scenario for 2100 is projected to be 2.50°C (Frölicher *et al.*, 2018). In this study, future MHW temperatures were projected by adding this maximum intensity to the future maximum SST. While MHWs can occur at any time of the year, this study focuses on assessing the most extreme conditions.

Statistical analysis

Physiological processes and performance

The analysis of variance (ANOVA) assumptions were checked using the Kolmogorov–Smirnov test for normality and Levene's test for equal variance. Two-way repeated measures ANOVA tests were conducted with the main factors being species and temperature and the time of measurement being the repeated factor, on chlorophyll fluorescence parameters (F_v/F_m , F_v/F_0 , and ϕ PSII), and RLC parameters (ETR_{max} , α , and E_k). The metabolism parameters (net oxygen production rate and respiration) and oxidation-related parameters (ROS, SOD, GPOX, and GSH) were tested with two-way ANOVA to examine the statistically significant effects of species and temperature. Lastly, one-way ANOVA tests were performed to investigate significant differences in pigments (chlorophyll *a*, chlorophyll *b*, and chlorophyll *c*) by temperature. Subsequently, after the ANOVA test, Fisher's least significant difference (LSD) was used to examine the differences between the species and the temperatures for all the parameters mentioned above.

Model fitting and selection

TPC were conducted in R Studio (v.4.4.1, R Core Team (2013)). The TPC models from the rTPC package (Padfield and O'Sullivan, 2023) were used to try to fit the data, and the models that do not follow the theoretical pattern of thermal responses were excluded. Four models (Gaussian_1987, Hinshelwood_1947, Modified gaussian_2006, and Thomas_2012) were chosen and the root mean square error (RMSE) and Akaike Information Criterion with a correction for finite sample sizes (AICc) were calculated (Padfield and O'Sullivan, 2023). The most suitable model for this study was chosen based on the minimum levels of RMSE and AICc. The 'hinshelwood_1947' model (Equation 5; Hinshelwood (1946), as cited in Padfield and O'Sullivan (2023)) was identified as the most suitable for this study (see Table S1) and was selected for further analysis.

$$R(T) = a \cdot \exp^{\frac{-e}{k \cdot (T+273.15)}} - b \cdot \exp^{\frac{-e_h}{k \cdot (T+273.15)}} \quad (5)$$

In the Hinshelwood_1947 equation, $R(T)$ is the biological rate at temperature T (°C). Here a is the rate constant for activation, b is the rate constant for de-activation, e is the activation energy, and e_h is the deactivation energy (Hinshelwood (1946), as cited in Padfield and O'Sullivan (2023)).

After the model fit, these parameters were extracted from the fitted-curve: R_{max} is the the maximum biological rate, T_{opt} (°C) is the temperature that allows the biological rate maximum, CT_{max} (°C) is the critical thermal maximum at which the biological rate was not above 0.1 of R_{max} , and the TSM is the range of supraoptimal temperature which the organism can still survive. TSM was calculated from the difference between CT_{max} and T_{opt} (Padfield and O'Sullivan, 2023).

Results

Chlorophyll fluorescence parameters

The maximum quantum yield (F_v/F_m) and the potential activity of PSII (F_v/F_0)

The level of F_v/F_m is mainly dependent on temperature level (two-way repeated measures ANOVA, $p < 0.001$), time of measurement ($p < 0.001$), and all interaction terms among the three factors ($p < 0.001$) (Table S2). The significant interactions between species and temperature ($p < 0.001$) indicate differences in the sensitivity of F_v/F_m by species. In non-extreme temperature (28–36°C), the change in F_v/F_m was not detected by all species (Fisher's LSD test). In contrast, at 40°C, all species exhibited a decrease in F_v/F_m (Fisher's LSD test), although these decreases varied by species. Thus, at the end of the experiment (48 h) in 40°C treatment, F_v/F_m in *P. boryana* were at a higher level than in *H. opuntia* and *H. macroloba* (Fisher's LSD test) (Figure 2A).

Using the same measurement as for F_v/F_m , F_v/F_0 showed a more dramatic change than F_v/F_m . F_v/F_0 was found to depend on species (two-way repeated measures ANOVA, $p < 0.001$), temperature level ($p < 0.001$), time of measurement ($p < 0.001$), and interactions between these terms ($p < 0.001$) (Table S2). Likely with F_v/F_m , species exhibited different thermal sensitivities from those in F_v/F_0 , which is indicated by the significant interactions between species and temperature ($p < 0.001$). Like F_v/F_m , the change in F_v/F_0 was also found at a high temperature of 40°C (Fisher's LSD test) with varied effects depending on the species. Then, at the end of the experiment (60 h), there was a significantly higher F_v/F_0 in *P. boryana* compared to *H. opuntia* and *H. macroloba* (Fisher's LSD test) (Figure 2B).

Effective quantum yield of PSII (ϕ PSII)

The level of ϕ PSII was found to depend on species (two-way repeated measures ANOVA, $p < 0.001$), temperature level (two-way repeated measures ANOVA, $p < 0.001$), time of measurement ($p < 0.001$), and interactions between these terms ($p < 0.001$) (Table S2). The thermal sensitivity of ϕ PSII was found to depend on species indicated by the significant interaction between species and temperature ($p < 0.001$). The change of ϕ PSII was found only at a high temperature of 40°C, which was statistically significant since 2 h of the stress phase and increasing over time in all studied species (Fisher's LSD test). This effect varied by species, with *P. boryana* consistently showing higher ϕ PSII levels than *H. opuntia* and *H. macroloba* until the end of the experiment (Fisher's LSD test) (Figure 3).

Rapid light curves

Results of the three parameters that were extracted from the RLCs show that α and E_k are dependent on temperature level (two-way repeated measures ANOVA, $p < 0.001$), time of measurement ($p < 0.001$), and the interaction term of the three factors ($p < 0.001$) (Table S3). The significant interactions between species

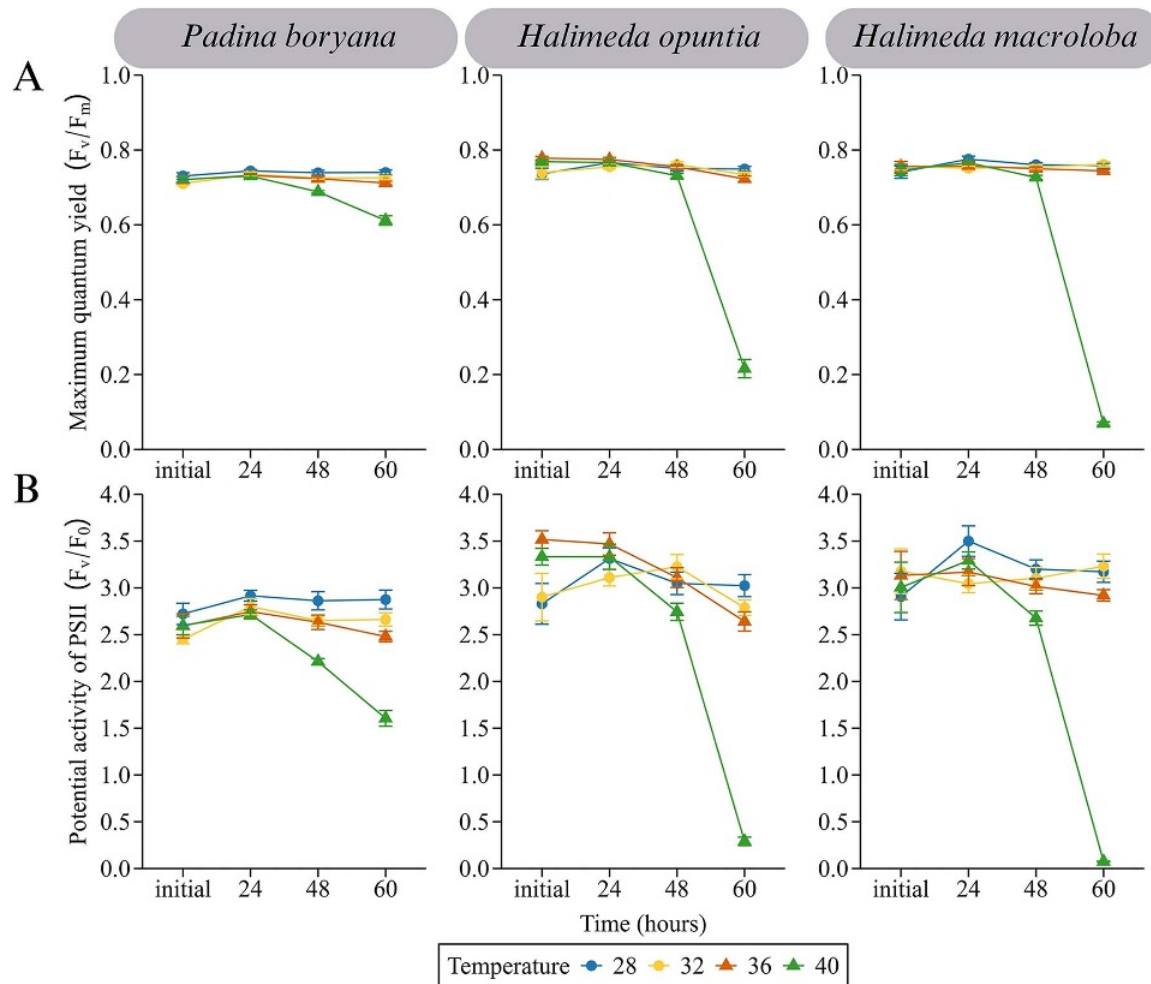


Figure 2. (A) Maximum quantum yield (F_v/F_m); (B) potential activity of PSII (F_v/F_0) of *Padina boryana*, *Halimeda opuntia*, and *H. macroloba* initially, then at 24 (before ramping phase), 48 (after ramping phase), and 60 h (end of experiment) of experiment in four temperature treatments (28°C, 32°C, 36°C, and 40°C). The error bars represent SE ($n = 12$).

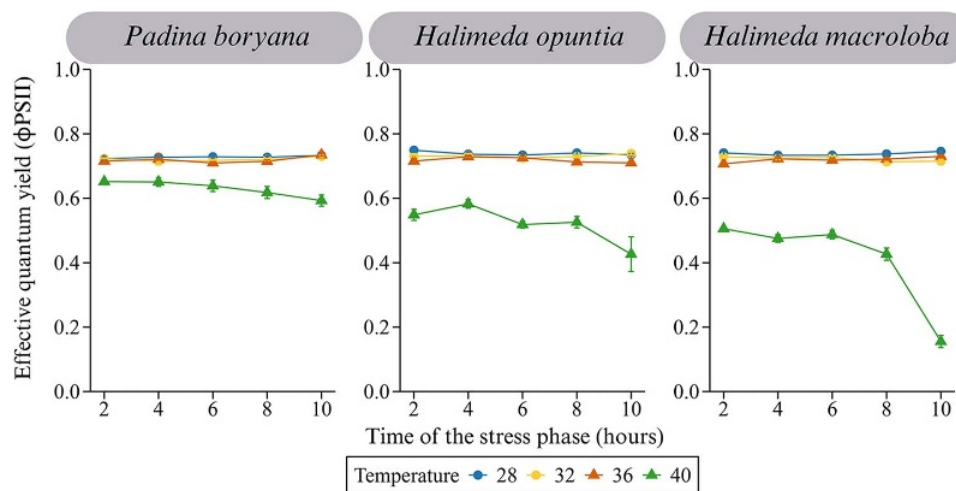


Figure 3. Effective quantum yields (ϕ_{PSII}) of *Padina boryana*, *Halimeda opuntia*, and *H. macroloba* at 2, 4, 6, 8, and 10 h of the stress phase in four temperature treatments (28°C, 32°C, 36°C, and 40°C). The error bars represent SE ($n = 12$).

and temperature ($p < 0.001$) suggest significant differences in thermal sensitivity among species. The changes of levels of α and E_k

among species were only observed at a temperature of 40°C, where α in both *Halimeda* species is lower than in *P. boryana* (Fisher's

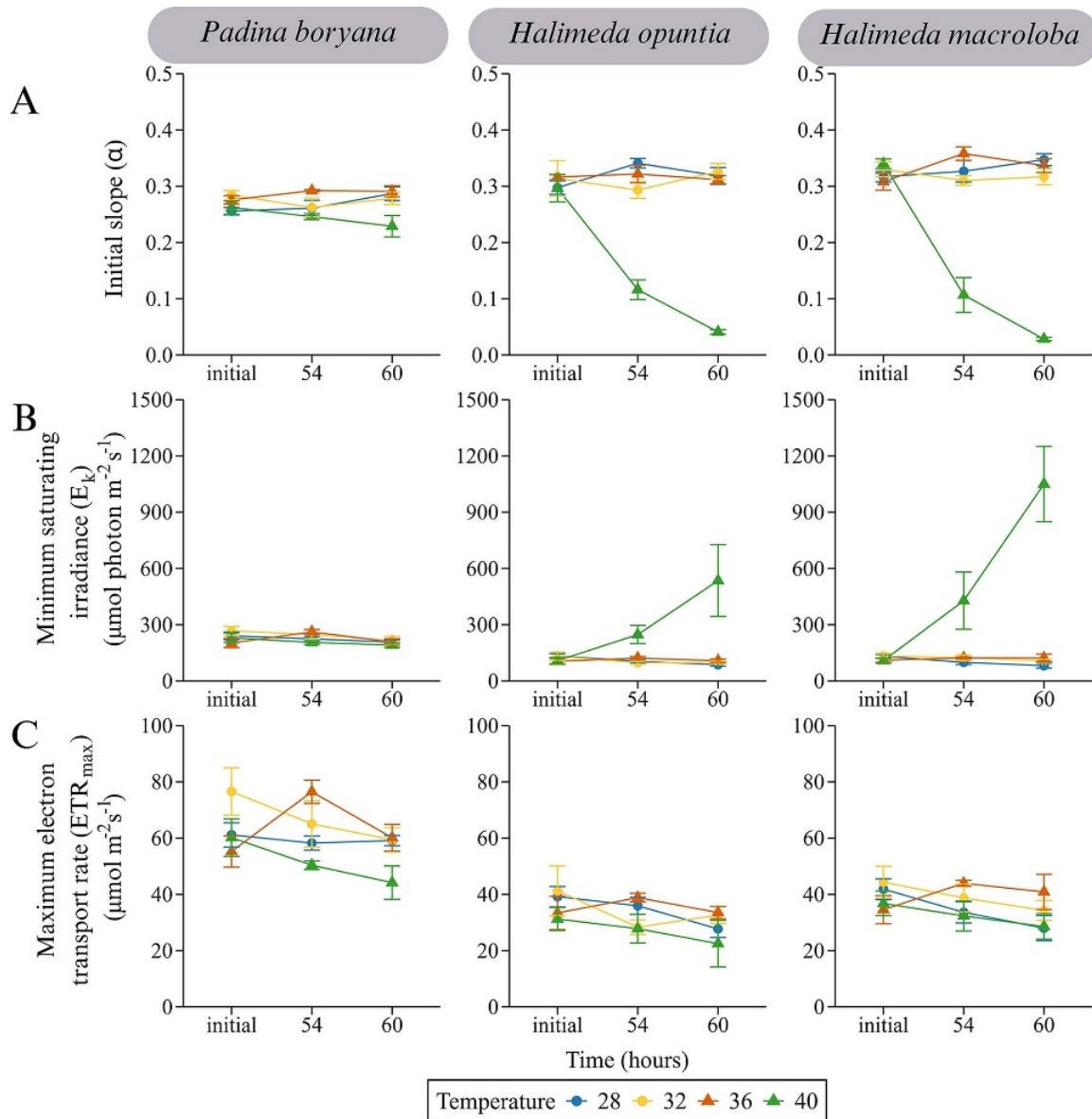


Figure 4. RLC parameter including (A) initial slope of RLC (α); (B) minimum saturating irradiance (E_k); and (C) maximum electron transport rate (ETR_{max}) of *Padina boryana*, *Halimeda opuntia*, and *H. macroloba* at initial, 54 (6 h after the stress phase), and 60 (12 h after the stress phase) h of experiment in four temperature treatments (28°C, 32°C, 36°C, and 40°C). The error bars represent SE ($n = 4$).

LSD test), which leads to a higher light requirement to reach their E_k (Fisher's LSD test) (Figure 4A and B).

In contrast to E_k and α , ETR_{max} is mainly influenced by species (two-way repeated measures ANOVA, $p < 0.001$) and temperature ($p < 0.001$) but not by the interactions between species and temperature ($p = 0.422$) (Table S3). This indicates that there were no significant differences in thermal sensitivity among species. However, *P. boryana* showed significantly higher ETR_{max} than both *Halimeda* species in all temperature conditions (Fisher's LSD test) (Figure 4C).

Metabolism

The net oxygen production rate was found to be dependent on species (two-way ANOVA, $p < 0.001$), temperature ($p < 0.001$), and interaction between species and temperature ($p < 0.001$)

(Table S4). In the non-extreme temperatures range (28–36°C), the net oxygen production rate in *P. boryana* is higher than in both *Halimeda* species (Fisher's LSD test). At the extreme temperature of 40°C, *P. boryana* exhibited a dramatic drop in net oxygen production compared to the lower temperature treatment (Fisher's LSD test). However, in all three studied species, the levels of net oxygen production rate at this high temperature are nearly zero (Figure 5A).

The respiration rate was also dependent on species (two-way ANOVA, $p < 0.001$), temperature ($p < 0.05$), and interaction between species and temperature ($p < 0.05$) (Table S4). The respiration rate in the non-extreme temperature range (28–36°C) of *P. boryana* is higher than in both *Halimeda* species, like the photosynthesis rates (Fisher's LSD test). However, an increase in the respiration rate due to high temperature was only found at 40°C in *H. opuntia* (Figure 5B).

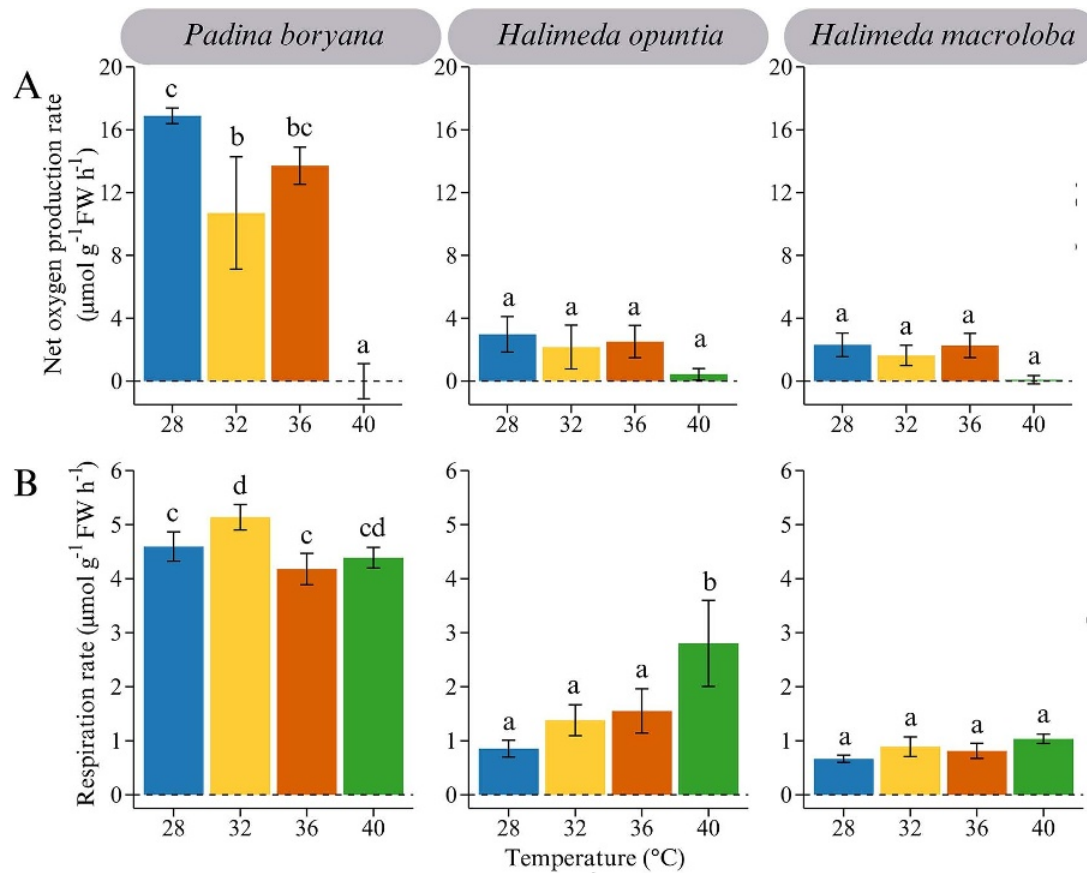


Figure 5. (A) Net oxygen production rate and (B) respiration rate of *Padina boryana*, *Halimeda opuntia*, and *H. macroloba* in 4 h of the stress phase in four temperature treatments (28°C, 32°C, 36°C, and 40°C). The error bars represent SE. Different letters above the bars indicate statistical significance in differences by species and temperature (Fisher's LSD test) ($n = 4$).

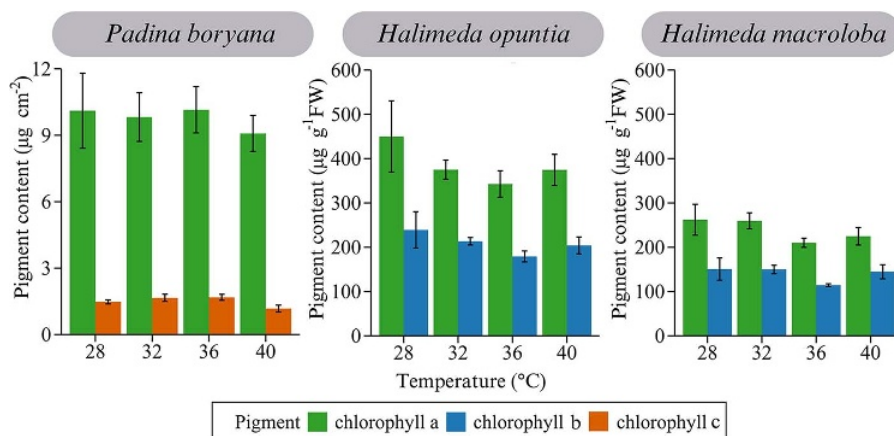


Figure 6. Pigment contents which include chlorophyll *a* and *c* of *Padina boryana*, and chlorophyll *a* and *b* of *Halimeda opuntia* and *H. macroloba* at the end of the experiment in four temperature treatments (28°C, 32°C, 36°C, and 40°C). The error bars represent SE ($n = 4$).

Pigment contents

Pigment analysis at the end of the experiment indicates that temperature levels did not significantly affect either chlorophyll *a* (one-way ANOVA, $p = 0.91$) or chlorophyll *c* ($p = 0.12$) in *P. boryana*. Similarly, in *Halimeda*, temperature levels did not significantly affect either chlorophyll *a* ($p = 0.61$ for *H. opuntia* and 0.62 for *H. macroloba*) or chlorophyll *b* ($p = 0.60$ for *H. opuntia* and 0.48 for *H. macroloba*) (Table S5, Figure 6).

Oxidative stress-related parameters

Levels of all oxidative stress-related parameters, e.g. total ROS, SOD activity, GPOX activity, and GSH content, were significantly different among species (two-way ANOVA, $p < 0.001$), temperature ($p < 0.001$), and the interaction between species and temperature ($p < 0.001$) (Table S6). Total ROS levels at lower temperatures (28–36°C) were higher in *H. opuntia* compared to the other two species (Fisher's LSD test). However, at 40°C, total ROS levels in

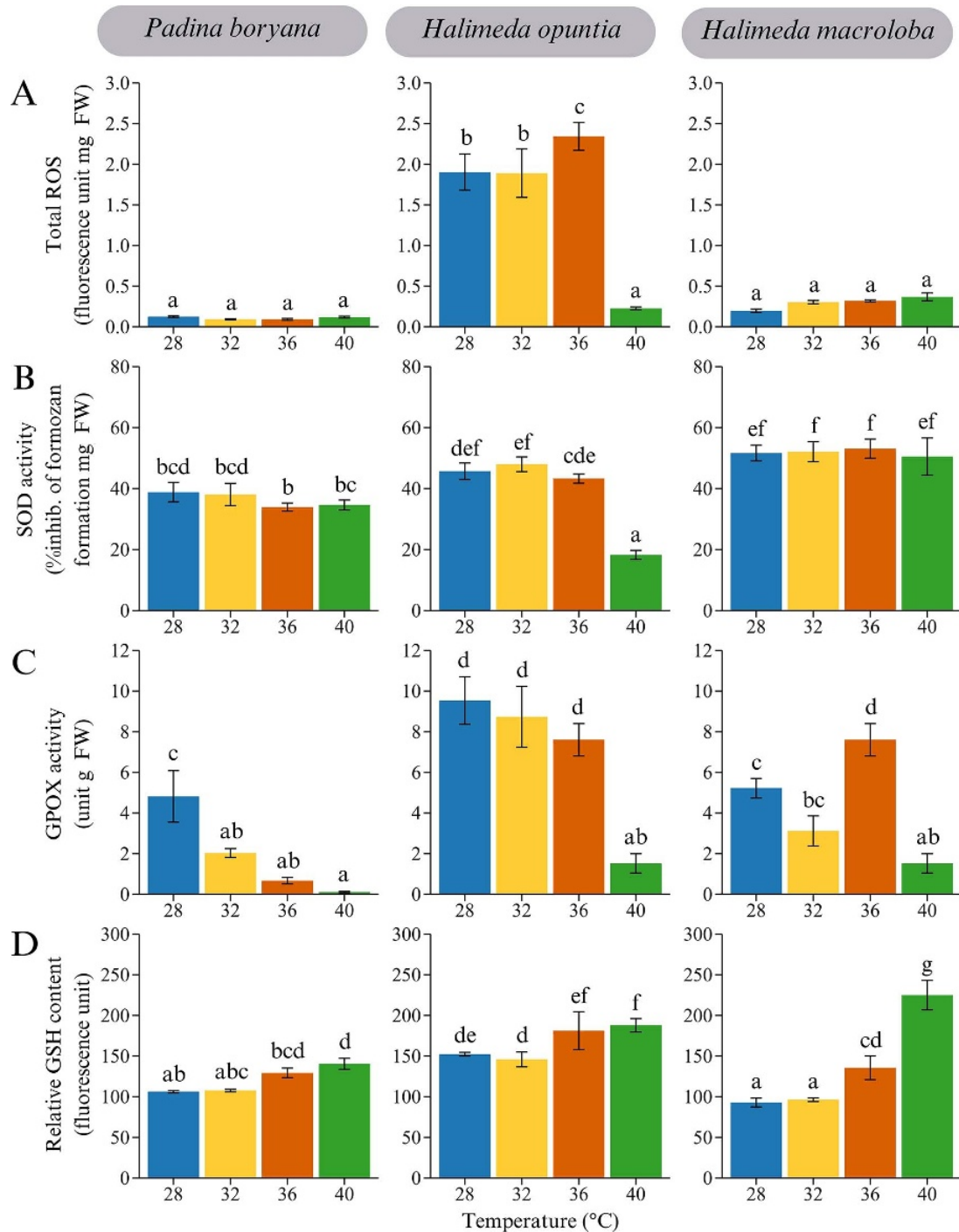


Figure 7. (A) Total reactive oxygen species (ROS); (B) superoxide dismutase (SOD) activity; (C) guaiacol peroxidase (GPOX) activity; and (D) glutathione (GSH) content of *Padina boryana*, *Halimeda opuntia*, and *H. macroloba* at the end of experiment in four temperature treatments (28°C, 32°C, 36°C, and 40°C). The error bars represent SE. Different letters indicate statistically significant differences by species and temperature (Fisher's LSD test) ($n = 4-12$).

H. opuntia dropped dramatically and matched the levels of the other two species (Fisher's LSD test) (Figure 7A). SOD activity in *P. boryana* was lower than in both *Halimeda* species at lower temperatures (28–36°C) (Fisher's LSD test). However, at 40°C, SOD activity in *H. opuntia* decreased significantly, while in the other two species, it remained similar to levels observed at lower

temperatures (Fisher's LSD test) (Figure 7B). GPOX activity in *H. opuntia* was higher compared to the other species at 28°C and 32°C (Fisher's LSD test). A significant drop in GPOX activity was observed in all studied species, with significant decreases found at 36°C in *P. boryana* and at 40°C in both *Halimeda* species. (Fisher's LSD test) (Figure 7C). Accumulation of GSH content was found at

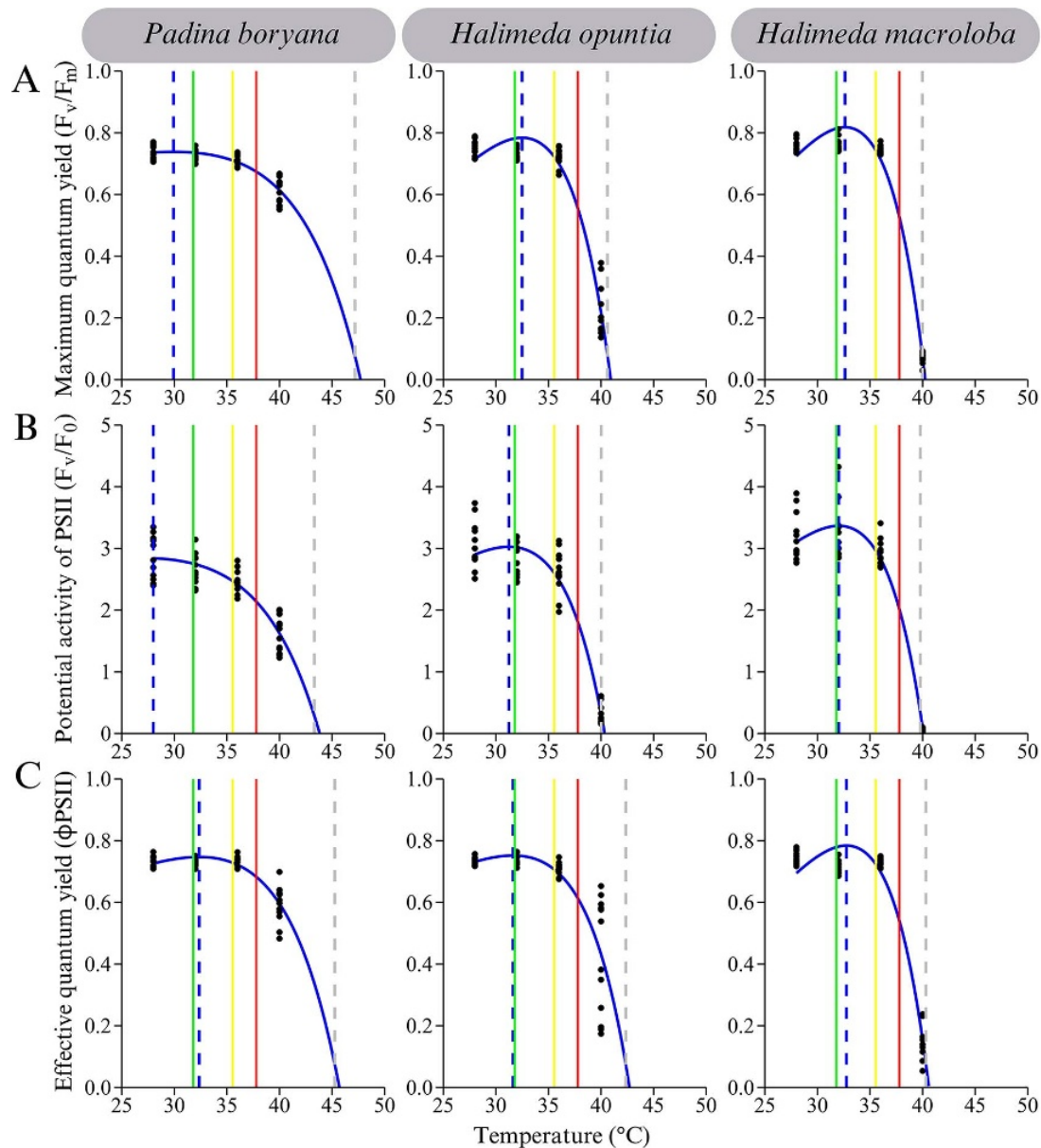


Figure 8. Thermal performance curves (TPCs) of (A) maximum quantum yield (F_v/F_m); (B) potential activity of PSII (F_v/F_0); and (C) effective quantum yield (ϕ PSII) of *Padina boryana*, *Halimeda opuntia*, and *H. macroloba* using hinshelwood_1947 model. The blue line represents TPC fit to data. The blue and grey vertical dash lines represent the optimum temperature (T_{opt}) and the critical temperature (CT_{max}), respectively. The green, yellow, and red solid lines represent the maximum current maximum sea surface temperature (SST), predicted future maximum SST and predicted maximum MHW temperature, respectively.

36°C and 40°C in *H. opuntia*, while in the other two species, it was observed at 40°C (Fisher's LSD test) (Figure 7D).

Thermal performance curve

The photosynthetic performance (F_v/F_m , F_v/F_0 , and ϕ PSII) and net oxygen production of the three studied macroalgal species exhibited a typical nonlinear relationship between temperature and biological rates and were fitted by the Hinshelwood_1947 model equation (Equation 5) (Table S1). In contrast, respiration rate did not fit the model in any of the tested species. Therefore, it was excluded from models reported because the fitting had no success.

The fitting model of photosynthetic performance revealed different thermal responses among species. From F_v/F_m and

F_v/F_0 fitting, optimal temperatures (T_{opt}) in *P. boryana* (29.91°C, 28.00°C) were at a lower temperature compared to *H. opuntia* (32.48°C, 31.23°C) and *H. macroloba* (32.62°C, 32.02°C). In contrast, T_{opt} values derived from ϕ PSII fittings were similar across species (~32°C). The critical thermal maximum (CT_{max}) derived from all photosynthesis parameters was obviously higher in *P. boryana* (47.18°C; F_v/F_m , 43.31°C; F_v/F_0 , 45.24°C; ϕ PSII), while *H. opuntia* (40.60°C; F_v/F_m , 40.01°C; F_v/F_0 , 42.35°C; ϕ PSII) and *H. macroloba* (39.97°C; F_v/F_m , 39.78°C; F_v/F_0 , 40.31°C; ϕ PSII) showed a lower level. This lower level of T_{opt} and higher level of CT_{max} in *P. boryana* resulted in a higher TSM in all photosynthesis parameters when compared to both *Halimeda* species (Figure 8, Table 1). The maximum SST in the current situation is 32.18°C, which is close to T_{opt} , causing a decrease of less than 3% from

Table 1. Model parameters of Thermal performance curve (TPC) of maximum quantum yield (F_v/F_m), and potential activity of PSII (F_v/F_0), effective quantum yield (ϕ PSII), and net oxygen production of *Padina boryana*, *Halimeda opuntia*, and *H. macroloba* using hinshelwood_1947 model

Species	Parameter	R_{max}	T_{opt} (°C)	CT_{max} (°C)	TSM (°C)
<i>Padina boryana</i>	F_v/F_m	0.73	29.91	47.18	17.26
	F_v/F_0	2.84	28.00	43.31	15.31
	ϕ PSII	0.74	32.36	45.24	12.88
	Net oxygen production	16.15 $\mu\text{mol g}^{-1}$ FW h^{-1}	30.08	40.01	9.92
<i>Halimeda opuntia</i>	F_v/F_m	0.78	32.48	40.60	8.11
	F_v/F_0	3.02	31.23	40.01	8.78
	ϕ PSII	0.75	31.62	42.35	10.72
	Net oxygen production	3.96 $\mu\text{mol g}^{-1}$ FW h^{-1}	30.84	40.06	9.21
<i>Halimeda macroloba</i>	F_v/F_m	0.81	32.62	39.97	7.35
	F_v/F_0	3.36	32.02	39.78	7.76
	ϕ PSII	0.78	32.75	40.31	7.55
	Net oxygen production	2.91 $\mu\text{mol g}^{-1}$ FW h^{-1}	32.29	40.16	7.86

R_{max} = Maximum rate, T_{opt} = optimum temperature, CT_{max} = critical temperature, TSM = thermal safety margin.

the maximum level in all species and parameters. At the projected future maximum SST of 35.54°C, the effects differ among species, with *P. boryana* showing only a 3–4% decrease in F_v/F_m and EQY, while both *Halimeda* is more affected with a 7–8% drop in these parameters. This difference becomes more stronger at maximum future MHW temperatures of 38.04°C, where *P. boryana* shows only a 10% decrease in F_v/F_m and EQY, while *Halimeda* drops by 20–40%. The fit model of net oxygen evolution rate provides less variation in response among the studied species. However, the T_{opt} in *H. macroloba* (32.29°C) is slightly higher than in *P. boryana* (30.08°C) and *H. opuntia* (30.84°C). While CT_{max} is at the same level in all three species at 40°C (Figure 9, Table 1). When evaluating the impact of maximum current SST, predicted future maximum SST, and predicted future MHW temperatures on net oxygen evolution rate, we observed minimal variation among species. Specifically, the maximum current SST is close to the optimum point, resulting in values near their maximum levels for all studied species. Both the maximum future MHW temperatures and predicted future SST affect the species similarly, with effects ranging from 10% to 20% for future maximum SST and 40% to 50% for future MHW temperatures.

Discussion

Temperature has been indicated as an important environmental factor affecting the metabolism of organisms. The results of this study support that statement, showing that elevated temperatures influence all the physiological parameters that we study. However, we also found differences in thermal sensitivity and thermal responses among the three species that we studied: *Padina boryana*, *Halimeda opuntia*, and *H. macroloba*.

The results on chlorophyll fluorescence parameters (photosynthetic performance parameters (F_v/F_m , F_v/F_0 , and ϕ PSII) and RLC parameters (ETR_{max} , α , and E_k)) suggest that temperature level and duration of thermal stress have a highly significant effect on the macroalgal responses and on damage during the stress period (Ji and Gao, 2023). Moreover, this result is also dependent on interaction between species, and temperature levels indicate that

the sensitivity is dependent on species. However, this difference is not seen clearly in the low temperature range from 28°C to 36°C. In contrast, at a temperature of 40°C, the effect of high temperatures was observed and revealed a difference in thermal sensitivities by species. Specifically, in *P. boryana*, F_v/F_m , F_v/F_0 , and ϕ PSII are slightly decreased, and RLC parameters remain unchanged at this temperature level. Conversely, both *Halimeda* species at the same temperature level show a dramatic drop in F_v/F_m , F_v/F_0 , and ϕ PSII and a significant change in RLC parameters where α was decreased and E_k was increased. This relatively low response of *P. boryana* when compared to both *Halimeda* species implies that *P. boryana* has a better thermal tolerance (Buapet and Sinutok, 2023). A thermal threshold in *P. boryana* in a current study (40°C) is also consistent with Yucharoen *et al.* (2021), who reported that this species exhibits a large decline in F_v/F_m and F_v/F_0 when incubated in seawater at 42°C. Previous studies also reported that high temperatures change the shape of the RLC, aligning with this study, specifically by reducing photoefficiency, which leads to a higher light saturation level (Buapet and Sinutok, 2023; Liu *et al.*, 2017; Shen *et al.*, 2016). This change in the shape of RLC and this decline of photosynthesis parameters (F_v/F_m , F_v/F_0 , and ϕ PSII) at high temperature stem from the inactivation, malfunction, or breakdown of temperature-sensitive photosynthesis proteins, such as D1, Rubisco, and Rubisco activase (Wijewardene *et al.*, 2021; Yamamoto *et al.*, 2008; Yamori and von Caemmerer S, 2009). A large proportion of this damage is intermediate with the accumulation of ROS that reduces the turnover rate of the D1 protein (Pospíšil, 2016). Additionally, the drop in ϕ PSII could also result from the upregulation of non-photochemical quenching, which can be induced by high temperatures (Figueroa *et al.*, 2019; Herdean *et al.*, 2023). Nonetheless, Buapet and Sinutok (2023) report that this same set of studied species shows reduced P_{max} after 5 days of incubation at high temperature, while this study did not detect this phenomenon. This difference in results may be due to differences in duration of stress, and this phenomenon might be a case of delayed response. It should be noted that the photosynthesis parameter, which uses the fluorescent technique in *Halimeda* during thermal stress, should be interpreted

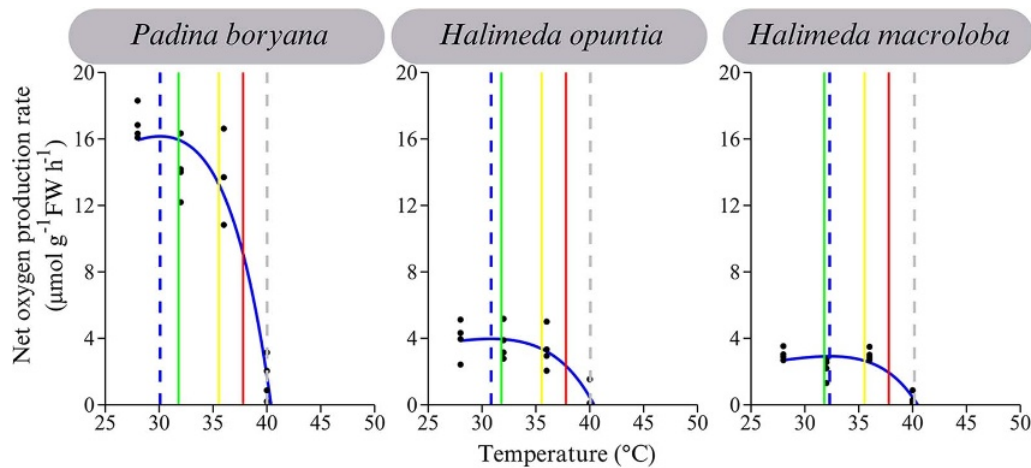


Figure 9. Thermal performance curves (TPCs) of net oxygen production rate of *Padina boryana*, *Halimeda opuntia*, and *H. macroloba* using hinshelwood_1947 model. The blue line represents the fit TPC. The blue and grey vertical dash lines represent the optimum temperature (T_{opt}) and the critical temperature (CT_{max}), respectively. The green, yellow, and red solid lines represent the maximum current maximum sea surface temperature (SST), predicted future maximum SST and predicted maximum MHW temperature, respectively.

with caution. This is because in this condition, *Halimeda* typically distributes chloroplasts to the inner part of tissue (Drew and Abel, 1990, 1992), and the photophysiology of them during this phenomenon is still elusive (Bhagooli *et al.*, 2022).

The results on chlorophyll content revealed that there was no change of chlorophyll pigment amount in their tissue even at high temperature in the current study. Conversely, Yucharoen *et al.* (2021) reported a significant decrease in total chlorophyll of *P. boryana* at 42°C treatment in a 5-day experiment. These studies suggest that the decrease in chlorophyll might be a delayed indicator of elevated temperature, and the 2 days like in the current study were not enough time for algae to respond or be damaged. Typically, the decrease in chlorophyll due to a high temperature is a result of chlorophyll degradation and the decrease in size and amount of the photosystem (Staehr and Wernberg, 2009; Wei *et al.*, 2020).

The results on the ROS in this current study, which does not detect the accumulation of ROS, suggest that the ROS scavenging system in all three studied species successfully copes with the ROS generation during stress. Especially in *H. macroloba*, where ROS drops at 40°C, which might be the result of activation of thermal defence mechanisms. On the other hand, Buapet and Sinutok (2023) indicate that there is a significant accumulation of ROS in *P. boryana* when faced with short-term high-temperature stress for 3 h. The difference in results between a short-term study (Buapet and Sinutok, 2023) and a longer-term study (current study) indicates the presence of thermal acclimation in the longer term in *P. boryana*. However, although the accumulation of ROS leads to the loss of photosynthesis efficiency (Ahumada-Fierro *et al.*, 2021; Czarnocka and Karpiński, 2018), some level of ROS is a normal situation since it is a by-product of the standard metabolism of oxygen activities (García-Caparrós *et al.*, 2021) and related to signalling (Zhao *et al.*, 2021). The results on oxidative stress-related parameters (SOD, GPOX, and GSH) revealed that the level and the change of ROS scavenging system characteristics during each temperature vary across species. However, the downregulated enzymatic ROS scavenging system activity (SOD and GPOX) was surprisingly found in all study species after incubating in seawater at a temperature of 40°C. Conversely, GSH content is upregulated in all studied species and may be mainly responsible for coping

with high temperature stress. Similarly, a proteome study in *Ulva prolifera* suggests that a high temperature induces upregulation in many stress response-related proteins, including GSH-related enzymes (Fan *et al.*, 2018). GSH is a non-enzymatic scavenger and can function as direct scavenger of ROS, but it also plays a key role in redox reaction of ascorbate–GSH pathway (Štolfa *et al.*, 2016).

The results of the net oxygen production rate indicate a dramatic decrease in photosynthesis at temperatures of 40°C, revealing that this level of temperature is beyond the upper limit for thermal stress. In contrast, no species exhibited a significant drop in respiration rate, revealing that the temperature threshold of respiration is higher than the maximum temperature employed in this study and higher than that for photosynthesis. The fact that photosynthesis responded more sensitively than respiration to high temperatures suggests that there is a difference in the thermal sensitivity of proteins that underlie each process (Ji *et al.*, 2016). In the current study, we found an increase in respiration due to high temperatures only in *H. opuntia*, suggesting that it plays a part in the decline of the net oxygen evolution rate. Conversely, in the other two species, this decrease in net oxygen evolution rate is solely explained by a reduction of photosynthetic rate. In addition to the direct effects of high temperature on photosynthetic and respiratory processes, it also influences gas solubility in seawater. As temperature increases, the solubility of gas decreases, leading to lower levels of dissolved oxygen and dissolved carbon dioxide, which may impact photosynthesis and respiration rates to some extent (Rasmusson *et al.*, 2020). This makes high-temperature events, such as MHWs, commonly linked to oxygen deficiency, especially in shallow areas (Safonova *et al.*, 2024). Photorespiration could also have an impact on the net oxygen production, but this must be less important in marine algae because of the presence of carbon concentration mechanisms (Ji and Gao, 2023; Li *et al.*, 2021).

The comparison among TPC models that are available in the rTPC package to fit thermal response on photosynthesis performance of (F_v/F_m , F_v/F_0 , and ϕ_{PSII}) and net oxygen production reveals that the Hinshelwood_1947 equation provides the best-fit curve and is the most biologically meaningful in all studied species. Even though the Hinshelwood_1947 equation was initially developed for plotting of enzyme kinetics versus temperature

(Hinshelwood, 1946, as cited in Padfield and O'Sullivan, 2023; Pasos-Panqueva *et al.*, 2024), this equation is one of the best models to fit TPC of photosynthetic parameters in photosynthetic organisms (Low-Décarie *et al.*, 2017). The best-fit parameter among studied parameters in this study was F_v/F_m followed by ϕ PSII and F_v/F_0 . This indicates that F_v/F_m is the highest precision parameter to predict by the model. Conversely, the net oxygen evolution rate parameter performed poorly in this study so its forecast should be used with caution. The exclusion of TPC of respiration due to the inability to achieve a good model fit in the current study might be the result of the linear relationship of respiration data. This unexpected phenomenon was also found in some studies that studied TPC of respiration in photosynthetic organisms (Anton *et al.*, 2020; Ji *et al.*, 2016).

The results of all parameters extracted from the TPC of photosynthesis parameters (F_v/F_m , F_v/F_0 , and ϕ PSII) suggest differences in thermal responses among the studied species. *P. boryana* has a little lower optimum temperature (T_{opt}) than *Halimeda* ($\sim 30^\circ\text{C}$ vs. $\sim 32^\circ\text{C}$) but a lot higher critical thermal maximum (CT_{max}) ($\sim 45^\circ\text{C}$ vs. $\sim 40^\circ\text{C}$). This leads *P. boryana* to having a lot larger TSM of 15°C compared to 8°C for both *Halimeda* species. These results can imply that *P. boryana* is better in tolerance to high temperatures and higher in resilience against seawater temperature fluctuations. This aligns with the temperature threshold in previous studies, where it is at 42°C in *P. boryana* (Yucharoen *et al.*, 2021), which is higher than that of *H. opuntia* at 36°C (Wei *et al.*, 2020). Contrary to the above results, TPCs on the oxygen evolution rate indicate that T_{opt} , CT_{max} , and TSM are approximately 31°C , 40°C , and 9°C , respectively, across all studied species. When comparing these parameters on net oxygen evolution rate with TPCs on photosynthesis parameters (F_v/F_m , F_v/F_0 , and ϕ PSII), both *Halimeda* reveal the same results, while for *P. boryana* the level is clearly different. It can be inferred that there is a difference in thermal responses between the two processes in *P. boryana*. The CT_{max} level of algae indicated by the current study is still higher than that of tropical coral, which was found to be only around 36.5°C (Silbiger *et al.*, 2019), indicating a relatively higher tolerance to high temperatures in algae compared to coral. Moreover, a field study also shows that macroalgae invade coral area after coral bleaching due to a heat stress event (Fukunaga *et al.*, 2022). It should be noted that the analysis of CT_{max} in this study relies on interpolation beyond the experimental data range, so the interpretation should be made with caution.

Temperature is one of the most important factors that limit the distribution of macroalgae (Des *et al.*, 2020; Khan *et al.*, 2018; Ramos *et al.*, 2020; Sjøtun *et al.*, 2015) since it has a large impact on their physiological processes (Román *et al.*, 2020). *P. boryana*, *H. opuntia*, and *H. macroloba* were found in the same location and depth at Tang Khen Bay, Phuket, Thailand (Buapet and Sinutok, 2021, 2023; Sinutok, 2008; Wichachucherd *et al.*, 2010), meaning that they are exposed to similar temperature ranges and face the same crisis. The analysis of the temperature crisis in this study shows that maximum current SST does not reduce their photosynthesis in all species and all parameters, indicating a high thermal tolerance in these species. However, in future maximum SST and maximum predicted MHW temperature, the effect was detected, indicating a potential stress condition. Nevertheless, these temperatures are still below CT_{max} , suggesting that they can still perform photosynthesis and still function as primary producers, but at a lower level than under normal conditions. The modeling of fluorescence photosynthesis

parameter also reveals that *P. boryana* demonstrates a superior capacity to maintain photosynthetic activity under conditions of high temperature stress compared to both *Halimeda* species, indicating a competitive advantage under this condition. Based on differences in thermal tolerance, it is predicted that during global warming, species with higher heat resistance will increase dominance (Somero, 2010). Consequently, in thermal stress conditions, *P. boryana*'s competitive advantage may facilitate its increased dominance within the community. However, this prediction should be interpreted with caution since other factors may also influence the actual response of these species (Somero, 2010).

While predictions on the effects of maximum temperatures from current maximum SST, future maximum SST, and future MHWs on photosynthesis suggest generally safe thermal conditions, these may not reflect the local temperatures in shallow waters where these species inhabit under such conditions. In shallow waters, local temperatures fluctuate more than in open water due to diel and tidal cycles (Mislán *et al.*, 2009). During the spring tide, if the tide recedes during midday to early afternoon, water temperatures can rapidly increase, exceeding 40°C (Yucharoen *et al.*, 2021). Consequently, these algae experience brief exposure to seawater at or near their CT_{max} . The global warming conditions like the increase in open water SST and the occurrence of MHWs might amplify the daily temperature fluctuations, pushing peak temperatures higher and extending the duration of extreme conditions (Wiberg, 2023). Therefore, projections of the effects of global warming based solely on predicted open water SST and MHWs may underestimate these algae actual impact on these conditions. Nonetheless, this study relies on these projections due to the lack of predicted shallow water temperature data during both phenomena.

It should be mentioned that the threshold and response found in this study cannot fully predict the threshold and response of future populations, since natural populations may adapt to better efficiency in coping with high temperatures due to natural selection after facing high SST and frequent heatwaves (Anton *et al.*, 2020; Somero, 2010). Furthermore, the results of this study do not fully explain all populations of studied species because intraspecific thermotolerance variations are common in macrophytes due to local adaptation (King *et al.*, 2018). So, the ability of adaptation to thermal change and intraspecific variation in thermotolerance in these species should be explored in future studies.

Overall, the results indicate that thermal stress significantly affects the photosynthetic performance, metabolism, and antioxidant responses of *P. boryana*, *H. opuntia*, and *H. macroloba*. Among the tested species, the results indicate that *P. boryana* has a relatively broader temperature range and relatively lesser thermal sensitivity than *H. opuntia* and *H. macroloba*. The variations observed in different parameters across species, temperatures, and time points highlight the complexity of their thermal responses and sensitivity. These findings contribute to a better understanding of the physiological and ecological responses of these macroalgae to changing temperature conditions, which is crucial for predicting their resilience to future climate change scenarios.

Supplementary material. The supplementary material for this article can be found at <https://doi.org/10.1017/S0025315425000359>.

Acknowledgements. We thank Coastal Oceanography and Climate Change Research Center and Faculty of Environmental Management, Prince of Songkla University, for research facilities. We gratefully acknowledge Dr. Pimchanok

Buapet for her insightful suggestions and valuable guidance, which have significantly contributed to the development of this research.

Author contributions. Conceptualization: PP, PC, SS. Data curation: PP, PC, MB, NT, SS. Formal analysis: PP, PC, NT, SS. Funding acquisition: PC, SS. Investigation: PP, PC, NT, SS. Methodology: PP, PC, SS. Project administration: PC, SS. Writing – original draft: PP, PC, MB, SS. Writing – review and editing: PP, PC, MB, NT, SS.

Funding. This work was supported by The National Science, Research and Innovation Fund (NSRF) and Prince of Songkla University (grant number: ENV6601152M).

Competing interests. The authors declare no conflict of interest.

References

- Ahumada-Fierro NV, García-Mendoza E, Sandoval-Gil JM and Band-Schmidt CJ (2021) Photosynthesis and photoprotection characteristics related to ROS production in three *Chattonella* (Raphidophyceae) species. *Journal of Phycology* 57, 941–954.
- Angilletta MJ, Cooper BS, Schuler MS and Boyles JG (2010) The evolution of thermal physiology in endotherms. *Frontiers in Bioscience E* 2, 861–881.
- Anton A, Randle JL, Garcia FC, Rossbach S, Ellis JJ, Weinzierl M and Duarte CM (2020) Differential thermal tolerance between algae and corals may trigger the proliferation of algae in coral reefs. *Global Change Biology* 26, 4316–4327.
- Babani F and Lichtenthaler HK (1996) Light-induced and age-dependent development of chloroplasts in etiolated barley leaves as visualized by determination of photosynthetic pigments, CO₂ assimilation rates and different kinds of chlorophyll fluorescence ratios. *Journal of Plant Physiology* 148, 555–566.
- Barati B, Gan S-Y, Lim P-E, Beardall J and Phang S-M (2019) Green algal molecular responses to temperature stress. *Acta Physiologiae Plantarum* 41, 26.
- Bennett S, Vaquer-Sunyer R, Jordá G, Forteza M, Roca G and Marbà N (2022) Thermal performance of seaweeds and seagrasses across a regional climate gradient. *Frontiers in Marine Science* 9. <https://doi.org/10.3389/fmars.2022.733315>.
- Bhagooli R, Soondur M, Ramah S, Gopeechund A, and Kaulysing D (2022) Variable photo-physiological performance of macroalgae and seagrasses from Saya de Malha and Nazareth Banks, Mascarene Plateau. *Western Indian Ocean Journal of Marine Science Special Issue 2/2021*, 95–108.
- Borowitzka MA and Larkum AWD (1987) Calcification in algae: mechanisms and the role of metabolism. *Critical Reviews in Plant Sciences* 6, 1–45.
- Buapet P and Sinutok S (2021) Calcification in three common calcified algae from Phuket, Thailand: potential relevance on seawater carbonate chemistry and link to photosynthetic process. *Plants* 10, 2537.
- Buapet P and Sinutok S (2023) Physiological responses to increased temperature and irradiance in the calcifying macroalgae, *Halimeda macroloba*, *Halimeda opuntia* and *Padina boryana*. *Applied Ecology and Environmental Research* 21, 4745–4780.
- Campbell J, Craft J, Muehllehner N, Langdon C and Paul V (2014) Responses of calcifying algae (*Halimeda* spp.) to ocean acidification: Implications for herbivores. *Marine Ecology Progress Series* 514, 43–56.
- Chintakovid N, Phaonakrop N, Surachat K, Phetcharat S, Wutiruk T, Roytrakul S and Mayakun J (2024) The proteome profile of *Halimeda macroloba* under elevated temperature: a case study from Thailand. *Journal of Marine Science and Engineering* 12, 1073.
- Clark JS, Poore AGB, Ralph PJ and Doblin MA (2013) Potential for adaptation in response to thermal stress in an intertidal macroalga. *Journal of Phycology* 49, 630–639.
- Crous KY, Uddling J and De Kauwe MG (2022) Temperature responses of photosynthesis and respiration in evergreen trees from boreal to tropical latitudes. *New Phytologist* 234, 353–374.
- Czarnocka W and Karpiński S (2018) Friend or foe? Reactive oxygen species production, scavenging and signaling in plant response to environmental stresses. *Free Radical Biology and Medicine* 122, 4–20.
- Das K and Roychoudhury A (2014) Reactive oxygen species (ROS) and response of antioxidants as ROS-scavengers during environmental stress in plants. *Frontiers in Environmental Science* 2. <https://doi.org/10.3389/fenvs.2014.00053>.
- Des M, Martínez B, deCastro M, Viejo RM, Sousa MC and Gómez-Gesteira M (2020) The impact of climate change on the geographical distribution of habitat-forming macroalgae in the Rías Baixas. *Marine Environmental Research* 161, 105074.
- Deutsch CA, Tewksbury JJ, Huey RB, Sheldon KS, Ghalambor CK, Haak DC and Martin PR (2008) Impacts of climate warming on terrestrial ectotherms across latitude. *Proceedings of the National Academy of Sciences* 105, 6668–6672.
- Díaz-Acosta L, Barreiro R, Provera I and Piñeiro-Corbeira C (2021) Physiological response to warming in intertidal macroalgae with different thermal affinity. *Marine Environmental Research* 169, 105350.
- Drew EA and Abel KM (1990) Studies on *Halimeda* III. A daily cycle of chloroplast migration within segments. *Botanica Marina* 33, 31–46.
- Drew EA and Abel KM (1992) Studies on *Halimeda* IV. An endogenous rhythm of chloroplast migration in the siphonous green alga, *H. distorta*. *Biological Rhythm Research* 23, 128–135.
- Duarte B, Martins I, Rosa R, Matos AR, Roleda MY, Reusch TBH, Engelen AH, Serrão EA, Pearson GA, Marques JC, Caçador I, Duarte CM, and Jueterbock A (2018) Climate change impacts on seagrass meadows and macroalgal forests: an integrative perspective on acclimation and adaptation potential. *Frontiers in Marine Science* 5, 190.
- Fan M, Sun X, Liao Z, Wang J, Li Y and Xu N (2018) Comparative proteomic analysis of *Ulva prolifera* response to high temperature stress. *Proteome Science* 16, 17.
- Fernández PA, Gaitán-Espitia JD, Leal PP, Schmid M, Reville AT and Hurd CL (2020) Nitrogen sufficiency enhances thermal tolerance in habitat-forming kelp: implications for acclimation under thermal stress. *Scientific Reports* 10, 3186.
- Figuerola FL, Celis-Plá PSM, Martínez B, Korbee N, Trilla A and Arenas F (2019) Yield losses and electron transport rate as indicators of thermal stress in *Fucus serratus* (Ochrophyta). *Algal Research* 41, 101560.
- Fredersdorf J, Müller R, Becker S, Wiencke C and Bischof K (2009) Interactive effects of radiation, temperature and salinity on different life history stages of the Arctic kelp *Alaria esculenta* (Phaeophyceae). *Oecologia* 160, 483–492.
- Frölicher TL, Fischer EM and Gruber N (2018) Marine heatwaves under global warming. *Nature* 560, 360–364.
- Fukunaga A, Burns JHR, Pascoe KH and Kosaki RK (2022) A remote coral reef shows macroalgal succession following a mass bleaching event. *Ecological Indicators* 142, 109175.
- García-Caparrós P, De Filippis L, Gul A, Hasanuzzaman M, Ozturk M, Altay V and Lao MT (2021) Oxidative stress and antioxidant metabolism under adverse environmental conditions: a review. *Botanical Review* 87, 421–466.
- Graba-Landry AC, Loffler Z, McClure EC, Pratchett MS and Hoey AS (2020) Impaired growth and survival of tropical macroalgae (*Sargassum* spp.) at elevated temperatures. *Coral Reefs* 39, 475–486.
- Hall JR, Albert G, Twigg IM, Baltar F, Hepburn CD, and Martin G (2022) The production of dissolved organic carbon by macroalgae and its consumption by marine bacteria: Implications for coastal ecosystems. *Frontiers in Marine Science* 9, 934229.
- Herdean A, Hall C, Hughes DJ, Kuzhiumparambil U, Diocaretz BC and Ralph PJ (2023) Temperature mapping of non-photochemical quenching in *Chlorella vulgaris*. *Photosynthesis Research* 155, 191–202.
- Hinshelwood CNS (1946) *The chemical kinetics of the bacterial cell*. Oxford, England: Oxford University Press.
- Hofmann L, Straub S and Bischof K (2012) Competition between calcifying and noncalcifying temperate marine macroalgae under elevated CO₂ levels. *Marine Ecology Progress Series* 464, 89–105.
- Jacobs JM, Himes L, and La Valle FF (2023) In situ carbon uptake of marine macrophytes is highly variable among species, taxa, and morphology. *Frontiers in Marine Science* 10, 1290054.
- Ji Y, and Gao K (2023) Responses of marine macroalgae to climate change drivers. In Kennish, MJ, Paerl, HW and Crosswell JR (eds), *Climate Change and Estuaries*. Florida, USA: CRC Press, pp. 335–354.

- Ji Y, Xu Z, Zou D and Gao K (2016) Ecophysiological responses of marine macroalgae to climate change factors. *Journal of Applied Phycology* **28**, 2953–2967.
- J P L Mur MEaSURES Project (2015) GHRSSST Level 4 MUR Global Foundation Sea Surface Temperature Analysis (v4. 1). PO. DAAC.
- Khan AH, Levac E, Van guelphen L, Pohle G and Chmura GL (2018) The effect of global climate change on the future distribution of economically important macroalgae (seaweeds) in the northwest Atlantic. *Facets* **3**, 275–286.
- King NG, McKeown NJ, Smale DA and Moore PJ (2018) The importance of phenotypic plasticity and local adaptation in driving intraspecific variability in thermal niches of marine macrophytes. *Ecography* **41**, 1469–1484.
- Koch M, Bowes G, Ross C and Zhang XH (2013) Climate change and ocean acidification effects on seagrasses and marine macroalgae. *Global Change Biology* **19**, 103–132.
- Kram SL, Price NN, Donham EM, Johnson MD, Kelly ELA, Hamilton SL and Smith JE (2016) Variable responses of temperate calcified and fleshy macroalgae to elevated pCO₂ and warming. *ICES Journal of Marine Science* **73**, 693–703.
- Li P, Liao Z, Zhou J, Yin L, Jiang HS and Li W (2021) Bicarbonate-use by aquatic macrophytes allows a reduction in photorespiration at low CO₂ concentrations. *Environmental and Experimental Botany* **188**, 104520.
- Liu C, Zou D, Yang Y, Chen B and Jiang H (2017) Temperature responses of pigment contents, chlorophyll fluorescence characteristics, and antioxidant defenses in *Gracilariaopsis lemaneiformis* (Gracilariales, Rhodophyta) under different CO₂ levels. *Journal of Applied Phycology* **29**, 983–991.
- Liu L, Zou D, Jiang H, Chen B and Zeng X (2018) Effects of increased CO₂ and temperature on the growth and photosynthesis in the marine macroalga *Gracilaria lemaneiformis* from the coastal waters of South China. *Journal of Applied Phycology* **30**, 1271–1280.
- Low-Décarie E, Boatman TG, Bennett N, Passfield W, Gavalás-Olea A, Siegel P and Geider RJ (2017) Predictions of response to temperature are contingent on model choice and data quality. *Ecology and Evolution* **7**, 10467–10481.
- Marín-Guirao L, Entrambasaguas L, Dattolo E, Ruiz JM and Procaccini G (2017) Molecular mechanisms behind the physiological resistance to intense transient warming in an iconic marine plant. *Frontiers in Plant Science* **8**, 1142.
- McNicholl C, Koch MS, Swarzenski PW, Oberhaensli FR, Taylor A, Batista MG and Metian M (2020) Ocean acidification effects on calcification and dissolution in tropical reef macroalgae. *Coral Reefs* **39**, 1635–1647.
- Mislan KAS, Wethey DS and Helmuth B (2009) When to worry about the weather: Role of tidal cycle in determining patterns of risk in intertidal ecosystems. *Global Change Biology* **15**(12), 3056–3065.
- Nelson WA (2009) Calcified macroalgae - critical to coastal ecosystems and vulnerable to change: A review. *Marine and Freshwater Research* **60**, 787.
- Nualla-ong A, Phongdara A and Buapet P (2020) Copper and zinc differentially affect root glutathione accumulation and phytochelatin synthase gene expression of *Rhizophora mucronata* seedlings: Implications for mechanisms underlying trace metal tolerance. *Ecotoxicology & Environmental Safety* **205**, 111175.
- Olivé I, Silva J, Costa MM and Santos R (2016) Estimating seagrass community metabolism using benthic chambers: The effect of incubation time. *Estuaries and Coasts* **39**, 138–144.
- Padfield D and O'Sullivan H (2023, August 17) rTPC: Fitting and analysing thermal performance curves. Available at <https://github.com/padpadpadpad/rTPC> (accessed 20 September 2024)
- Pasos-Panqueva J, Baker A and Camargo-Valero MA (2024) Unravelling the impact of light, temperature and nutrient dynamics on duckweed growth: A meta-analysis study. *Journal of Environmental Management* **366**, 121721.
- Phandee S, Hwan-air W, Soonthornkalump S, Jenke M and Buapet P (2022) Experimental flooding modifies rhizosphere conditions, induces photoacclimation and promotes antioxidant activities in *Rhizophora mucronata* seedlings. *Botanica Marina* **65**, 1–12.
- Pospišil P (2016) Production of reactive oxygen species by photosystem II as a response to light and temperature stress. *Frontiers in Plant Science* **7**. <https://doi.org/10.3389/fpls.2016.01950>.
- Ralph PJ and Gademann R (2005) Rapid light curves: A powerful tool to assess photosynthetic activity. *Aquatic Botany* **82**, 222–237.
- Ramos E, Guinda X, Puente A, de la Hoz CF and Juanes JA (2020) Changes in the distribution of intertidal macroalgae along a longitudinal gradient in the northern coast of Spain. *Marine Environmental Research* **157**, 104930.
- Rasmusson LM, Buapet P, George R, Gullström M, Gunnarsson PC and Björk M (2020) Effects of temperature and hypoxia on respiration, photorespiration, and photosynthesis of seagrass leaves from contrasting temperature regimes. *ICES Journal of Marine Science* **77**(6), 2056–2065.
- Rautenberger R, Huovinen P and Gómez I (2015) Effects of increased seawater temperature on UV tolerance of Antarctic marine macroalgae. *Marine Biology* **162**, 1087–1097.
- R Core Team (2013) R: A language and environment for statistical computing. *Foundation for Statistical Computing, Vienna, Austria*.
- Rebolledo AP, Sgrò CM, and Monro K (2021) Thermal performance curves are shaped by prior thermal environment in early life. *Frontiers in Physiology* **12**, 738338.
- Ritchie RJ (2006) Consistent sets of spectrophotometric chlorophyll equations for acetone, methanol and ethanol solvents. *Photosynthesis Research* **89**, 27–41.
- Román M, Román S, Vázquez E, Troncoso J and Olabarria C (2020) Heatwaves during low tide are critical for the physiological performance of intertidal macroalgae under global warming scenarios. *Scientific Reports* **10**(1), 1–14.
- Saewong C, Soonthornkalump S and Buapet P (2022) Combined effects of high irradiance and temperature on the photosynthetic and antioxidant responses of *Thalassia hemprichii* and *Halophila ovalis*. *Botanica Marina* **65**, 325–335.
- Safonova K, Meier HM and Gröger M (2024) Summer heatwaves on the Baltic Sea seabed contribute to oxygen deficiency in shallow areas. *Communications Earth & Environment* **5**(1), 106.
- Savva I, Bennett S, Roca G, Jordà G and Marbà N (2018) Thermal tolerance of Mediterranean marine macrophytes: Vulnerability to global warming. *Ecology and Evolution* **8**, 12032–12043.
- Scafetta N (2024) Impacts and risks of “realistic” global warming projections for the 21st century. *Geoscience Frontiers* **15**, 101774.
- Scherner F, Pereira CM, Duarte G, Horta PA, Castro CB, Barufi JB and Pereira SMB (2016) Effects of ocean acidification and temperature increases on the photosynthesis of tropical reef calcified macroalgae. *PLoS One* **11**, e0154844.
- Schreiber U (2004) Pulse-Amplitude-Modulation (PAM) fluorometry and saturation pulse method: An overview. In Christos PG and Govindjee (eds), *Chlorophyll A Fluorescence: A Signature of Photosynthesis*. Dordrecht: Springer Netherlands, pp. 279–319.
- Schulte PM, Healy TM and Fangue NA (2011) Thermal performance curves, phenotypic plasticity, and the time scales of temperature exposure. *Integrative and Comparative Biology* **51**, 691–702.
- Shen A, Ma Z, Jiang K and Li D (2016) Effects of temperature on growth, photophysiology, Rubisco gene expression in *Prorocentrum donghaiense* and *Karenia mikimotoi*. *Ocean Science Journal* **51**, 581–589.
- Silbiger NJ, Goodbody-Gringley G, Bruno JF and Putnam HM (2019) Comparative thermal performance of the reef-building coral *Orbicella franksi* at its latitudinal range limits. *Marine Biology* **166**, 126.
- Sinclair BJ, Marshall KE, Sewell MA, Levesque DL, Willett CS, Slotsbo S, Dong Y, Harley CDG, Marshall DJ, Helmuth BS and Huey RB (2016) Can we predict ectotherm responses to climate change using thermal performance curves and body temperatures? *Ecology Letters* **19**, 1372–1385.
- Sinutok S (2008) Seasonal variation in distribution, density, and life stage of *Halimeda macroloba* decaisne at Tangkhen Bay, Phuket Province, Thailand. M. Sc. Prince of Songkla University, Songkhla.
- Sjotun K, Husa V, Asplin L and Sandvik AD (2015) Climatic and environmental factors influencing occurrence and distribution of macroalgae a fjord gradient revisited. *Marine Ecology Progress Series* **532**, 73–88.
- Somero GN (2010) The physiology of climate change: How potentials for acclimatization and genetic adaptation will determine ‘winners’ and ‘losers’. *Journal of Experimental Biology* **213**(6), 912–920.

- Staehr PA and Wernberg T** (2009) Physiological responses of *Ecklonia radiata* (Laminariales) to a latitudinal gradient in ocean temperature¹. *Journal of Phycology* **45**, 91–99.
- Štolfa I, Špoljarić Maronić D, Pfeiffer TŽ and Lončarić Z** (2016) Glutathione and related enzymes in response to abiotic stress. In Gupta Dharmendra K, Palma José M and Corpas Francisco J (eds), *Redox State as a Central Regulator of Plant-Cell Stress Responses*. Cham: Springer International Publishing, pp. 183–211.
- Vasseur DA, DeLong JP, Gilbert B, Greig HS, Harley CDG, McCann KS, Savage V, Tunney TD and O'Connor MI** (2014) Increased temperature variation poses a greater risk to species than climate warming. *Proceedings of the Royal Society B: Biological Sciences* **281**, 20132612.
- Wei Z, Mo J, Huang R, Hu Q, Long C, Ding D, Yang F and Long L** (2020) Physiological performance of three calcifying green macroalgae *Halimeda* species in response to altered seawater temperatures. *Acta Oceanologica Sinica* **39**, 89–100.
- Wiberg PL** (2023) Temperature amplification and marine heatwave alteration in shallow coastal bays. *Frontiers in Marine Science* **10**, 1129295.
- Wichachucherd B, Liddle LB and Prathep A** (2010) Population structure, recruitment, and succession of the brown alga, *Padina boryana* Thivy (Dictyotales, Heterokontophyta), at an exposed shore of Sirinart National Park and a sheltered area of Tang Khen Bay, Phuket Province, Thailand. *Aquatic Botany* **92**, 93–98.
- Wieters EA, Medrano A and Quiroga G** (2013) Spatial variation in photosynthetic recovery of intertidal turf algae from acute UVB and temperature stress associated with low tides along the central coast of Chile. *Journal of Experimental Marine Biology and Ecology* **449**, 340–348.
- Wijewardene I, Shen G and Zhang H** (2021) Enhancing crop yield by using Rubisco Activase to improve photosynthesis under elevated temperatures. *Stress Biology* **1**(1), 1–20.
- Wu T, Xia L, Zhuang M, Pan J, Liu J, Dai W, Zhao Z, Zhang M, Shen X, He P, Zhang J and Qin Y** (2022) Effects of global warming on the growth and proliferation of attached *Sargassum horneri* in the aquaculture area near Gouqi Island, China. *Journal of Marine Science and Engineering* **11**, 9.
- Yamamoto Y, Aminaka R, Yoshioka M, Khatoon M, Komayana K, Takenaka D, Yamashita D, Nijo N, Inagawa K, Morita N, Sasaki T and Yamamoto Y** (2008) Quality control of photosystem II: Impact of light and heat stresses. *Photosynthesis Research* **98**(1), 589–608.
- Yamori W and von Caemmerer S** (2009) Effect of rubisco activase deficiency on the temperature response of CO₂ assimilation rate and rubisco activation state: insights from transgenic tobacco with reduced amounts of rubisco activase. *Plant Physiology* **151**, 2073–2082.
- Yucharoen M, Sinutok S, Chotikarn P and Buapet P** (2021) Experimental assessment of vulnerability to warming in tropical shallow-water marine organisms. *Frontiers in Marine Science* **8**, 767628.
- Zanolla M, Carmona R, Kawai H, Stengel DB and Altamirano M** (2019) Role of thermal photosynthetic plasticity in the dispersal and settlement of two global green tide formers: *Ulva pertusa* and *U. ohnoi*. *Marine Biology* **166**, 123.
- Zhao X, Zheng W, Qu T, Zhong Y, Xu J, Jiang Y, Zhang H, Tang X and Wang Y** (2021) Dual roles of reactive oxygen species in intertidal macroalgae *Ulva prolifera* under ultraviolet-B radiation. *Environmental and Experimental Botany* **189**, 104534.
- Zou D and Gao K** (2013) Thermal acclimation of respiration and photosynthesis in the marine macroalga *Gracilaria lemaneiformis* (Gracilariales, Rhodophyta). *Journal of Phycology* **49**, 61–68.
- Zou X-X, Xing S-S, Su X, Zhu J, Huang H-Q and Bao S-X** (2018) The effects of temperature, salinity and irradiance upon the growth of *Sargassum polycystum* C. Agardh (Phaeophyceae). *Journal of Applied Phycology* **30**, 1207–1215.